Acta Polytechnica **63**(3):179–187, 2023
https://doi.org/10.14311/AP.2023.63.0179

Published by the Czech Technical University in Prague

NEURAL NETWORK BASED PATIENT RECOVERY ESTIMATION OF A PAM-BASED REHABILITATION ROBOT

Van-Vuong Dinh, Minh-Chien Trinh, Tien-Dat Bui, Minh-Duc Duong, Quy-Thinh Dao*

Hanoi University of Science and Technology, School of Electrical and Electronic Engineering, 11615 Hanoi, Vietnam

* corresponding author: thinh.daoquy@hust.edu.vn

Abstract. Rehabilitation robots have shown a promise in aiding patient recovery by supporting them in repetitive, systematic training sessions. A critical factor in the success of such training is the patient's recovery progress, which can guide suitable treatment plans and reduce recovery time. In this study, a neural network-based approach is proposed to estimate the patient's recovery, which can aid in the development of an assist-as-needed training strategy for the gait training system. Experimental results show that the proposed method can accurately estimate the external torques generated by the patient to determine their recovery. The estimated patient recovery is used for an impedance control of a 2-DOF robotic orthosis powered by pneumatic artificial muscles, which improves the robot joint compliance coefficients and makes the patient more comfortable and confident during rehabilitation exercises.

Keywords: Pneumatic artificial muscle, rehabilitation robot, neural network, patient recovery.

1. Introduction

Nowadays, robots appear everywhere and play an essential role in many fields, such as industry, military, transportation and rescue service areas. With the increasing number of older people and the lack of physicians and nurses, robots are expected to assist and replace humans in healthcare and daily life. Healthcare and service robot systems have been the subject of extensive research in recent years [1, 2]. Currently, the majority of gait training systems commercially available utilise electric motors as actuators. However, these systems are associated with significant concerns, such as high costs and a low power/weight ratio of the motorised actuators. As an alternative, the pneumatic artificial muscle (PAM) system has been proposed due to its advantages, including a large power/weight ratio, low cost, lightweight, and similar characteristics to human muscles, as reported in recent studies [3–8]. For this reason, a many PAM-based gait training systems have been developed in the literature [8–16] that can assist the patient with movement according to the exercises prescribed by the physiotherapist.

Compared to other robot systems, the main differences of rehabilitation robots are the safety and the capability to improve the patient's recovery. Thus, the interactive force/moment between the robot and the human is required. To obtain force/moment information, one can usually use force/torque sensors, mainly used in rehabilitation robot systems. However, the external force/moment estimation without sensors is considered due to the cost and complicated assembly. Various studies have been conducted to estimate the external force acting on industrial robots [17–20]. In [17], a task-oriented dynamics model learning and a robust disturbance state observer are proposed. Force estimation based on machine learning is developed in [18, 20]. In addition, Cartesian contact force estimation for robotic manipulators using Kalman filter and the generalised momentum is reported in [19]. These methods are all for industrial robots and give good external force estimation results. However, they require the robot's dynamics and are pretty complicated, resulting in a difficult implementation.

One better solution for the estimation of external contact force is to use a neural network [21–24]. These researches consider two estimation approaches. The first approach is to estimate the contact force directly from the robot's motion information using a neural network [21]. The second approach is to estimate the robot's inverse dynamic model [22–24]. Then, the contact force is calculated by the difference between the robot actuator's torques for the case of contact force and without contact force. The disadvantage of the first approach is that the measurement of contact force is required for offline training of Neural Network. In contrast, the contact force measurement in the second approach is not required since the inverse dynamic model can be estimated in the free-motion condition. For this reason, the second approach is promising to estimate external force for rehabilitation robot. It leads to the estimation of the patient recovery in a training process.

In gait training robot systems, the estimation of patient interaction forces can bring many benefits. At first, this contact force can be used for the compliant control, patient-cooperative control, assist-as-needed

(AAN) that is required in rehabilitation exercises [8], together with trajectory tracking control. In addition, the contact force information can help the physician evaluate the patient's recovery during the treatment. The patient's interaction force can be measured directly, using force/torque sensors [8], but the installation is complicated and may cause a physical discomfort the patients. Another way to estimate the interaction force is to use Electromyography (EMG) signals of the patient's muscles [25]. EMG signals can be used to calculate the muscle force and supply the valuable muscle health information for a diagnosis and analysis of the patient's recovery. Nevertheless, the EMG measurement setup is complicated, and EMG signals vary with the patient's condition and time. Thus, the use of EMG signal may not be appropriate at present.

To overcome the limitation of contact force- and EMG-based approaches and fully utilise the advantages of the neural network based one, this research develops a simple and online method for estimating the external force of the PAM-based gait training robot. Instead of the force sensor as most gait training robots, this paper calculates the external force from forces generated by PAM actuators and the robot inverse dynamic. Since the rehabilitation robot has a complex structure, the determination of robot parameters is very complicated and inaccurate. This paper proposes a method for estimating joint torques using a neural network, which allows for an easy collection of training data in a robot free-motion mode. The estimated joint torques are then used to obtain the external force exerted by the patient, which is subsequently used for the impedance control of a PAM-based gait training system. In summery, the main contributions of the paper are:

- Using a neural network to estimate both the joint torques required to guide the robot during gait training and the external force generated by the patient, without the need for an external force measurement.
- The estimated patient's recovery is used for the impedance control of the PAM-based gait training system, improving the robot joint compliance coefficients and making the patient more comfortable and confident in their rehabilitation exercise.
- The proposed method offers a simpler and more practical approach to estimating the patient's recovery as compared to previous methods.
- The experimental results demonstrate the effectiveness of the proposed method for estimating the patient's recovery and improving the gait training robot system.

The rest of the paper is organised as follows. Section 2 presents the structure of the 2-DOF prototype exoskeletal robot for lower limb rehabilitation. The force estimation is demonstrated in Section 3. Section 4 presents the compliant control for the rehabilitation robot using the estimated patient's force. Conclusion and further studies are shown in Section 5.

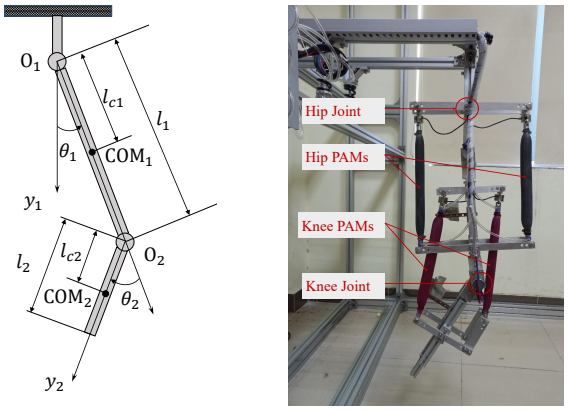

(A). (B).

Figure 1. The proposed method's experimental rig, with a typical 2-DOF robot (A) and a BK-Gait PAM-based lower limb orthosis (B) with COM representing the centre of mass.

2. Lower Limb Rehabilitation Robot System

This paper considers a BK-Gait based lower limb rehabilitation system for the experimental works. The system's main advantage is the suspension frame's direct attachment to the pre-shaped aluminum, which fixes the robot and lifts the patient to the desired height. The prototype robot is a 2-DOF robot, as shown in Figure 1a, which drives the lower limb of the subject with the help of two aluminum braces attached to the thigh and shank parts. The length of the robot's links can be adjusted based on the subjects' body using the slider located between the hip and knee joints. The hip and knee joints can flex/extend to a maximum angle of $-45°/+45°$ and $0°/90°$, respectively. Overall, the system's design allows for a customisable and effective rehabilitation experience for lower limb patients. The developed robotic exoskeleton system is depicted in the actual image shown in Figure 1b.

The robot system consists of two opposing muscles and joints fixed on a flat surface to enable the movement. The used PAM type is a McKibben artificial muscle, 2.5 cm in diameter. This PAM also has a maximum contraction rate of 30 % compared to muscle length similar to human muscles. We used two pairs of pressure regulators ITV-2030-212S-X26 by SMC in the developed muscle system. A pressure difference between the two control valves causes one muscle to contract and the other to stretch. That creates a rotation angle of the corresponding joint. A potentiometer WDD35D8 that ranges up to 360° is attached to each robot joint to measure the joint's position. Load cells are attached to the muscle's ends to measure the pull force of muscles. The NI Myrio platform developed by National Instrument was adopted to implement

the control algorithm. NI Myrio also collects voltage signals from load cells, potentiometers, and provides control signals. The control algorithm is developed and compiled in the Labview software environment before being downloaded to NI Myrio for a real-time control.

3. Human Torque Estimation

Let us consider the developed 2-DOF rehabilitation robot which has a typical schematic diagram in Figure 1a. When a torque vector M is applied to the robot system, the robot is moved with position vector q, and the dynamics of a robot system can be expressed as [26]:

$$M = H(q)\ddot{q} + V(q,\dot{q}) + G(q)\,, \tag{1}$$

where
$q = \begin{bmatrix} \theta_1 \\ \theta_2 \end{bmatrix}$ is the robot's position vector with θ_1 being the hip joint's angle and θ_2 the knee joint's angle.
$H(q) = \begin{bmatrix} h_{11} & h_{12} \\ h_{21} & h_{22} \end{bmatrix}$ is the inertia matrix.
$V(q,\dot{q}) = \begin{bmatrix} -m_2 l_1 l_{c2} \dot{\theta}_2 (2\dot{\theta}_1 + \dot{\theta}_2) \sin\theta_2 \\ m_2 l_1 l_{c2} \sin\theta_2 \dot{\theta}_1^2 \end{bmatrix}$ is the coriolis and centrifugal forces.

$G(q) = \begin{bmatrix} (m_1 l_{c1} + m_2 l_1) g \cos\theta_1 + m_2 l_{c2} \cos(\theta_1 + \theta_2) \\ m_2 g l_{c2} \cos(\theta_1 + \theta_2) \end{bmatrix}$
is the gravitational force vector.
$h_{11} = m_1 l_{c1}^2 + m_2(l_1^2 + l_{c2}^2 + 2 l_1 l_{c2} \cos\theta_2)$
$h_{12} = h_{21} = m_2(l_{c2}^2 + l_1 l_{c2} \cos\theta_2)$
$h_{22} = m_2 l_{c2}^2$ In the above equations, l_i and m_i $(i = 1, 2)$ are the length and mass of the robot's links; l_{ci} $(i = 1, 2)$ is the distances of the robot link's centre of mass from the respective joint rotation point. Table 1 shows the geometric parameters of the BK-Gait robot.

Parameters	l_1[m]	m_1[kg]	l_2[m]	m_2[kg]
Value	0.4	3.0	0.38	2.2

Table 1. Geometric parameters of the BK-Gait robot.

When the robot moves with an object (human), the total torques M impact the robot's joints, including two components: the torque generated by PAMs and the torque generated by the human.

$$M = M_{PAM} + M_{HM}\,, \tag{2}$$

where M_{PAM} is the PAM torque vector generated by PAMs and M_{HM} is the human torque vector generated by the human muscles. Then, the human torque (M_{HM}) can be calculated as:

$$M_{HM} = M - M_{PAM}\,. \tag{3}$$

The PAM torque (M_{PAM}) can be calculated from the force generated by the PAM, which is measured by the load cell mounted on each PAM. The joint torque (M) can be calculated based on the robot's inverse dynamics from Equation (1), theoretically. However, in practice, the precise calculation of the robot's joint torques is complicated since the determination of coefficients in $H(q)$, $V(q,\dot{q})$, and $G(q)$ is very complicated and less precise. This research uses a neural network to approximate the joint torque M to overcome this difficulty. The estimation of the human torque $\hat{M}_{HM}$ can be computed from the approximated torques of the neural networks M_{NN} as:

$$\hat{M}_{HM} = M_{NN} - M_{PAM}\,. \tag{4}$$

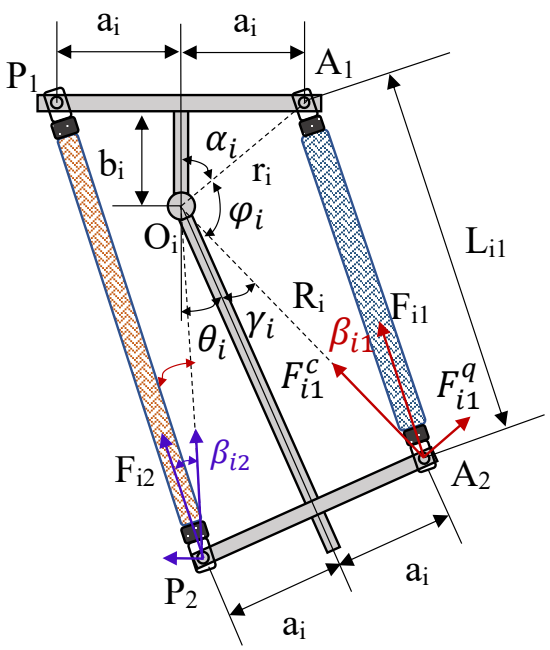

Figure 2. Geometric of the joint based on the antagonistic configuration of two PAMs.

3.1. Calculating the torque generated by PAMs (M_{PAM})

Consider the geometric model of a robot joint in Figure 2. In this figure, F_{ij} are the forces generated by the anterior and posterior PAMs of joint i, and $j = 1, 2$ represents the anterior and posterior PAMs. R_i is the rotation radius of the joint. M_i is the moment of anterior and posterior PAMs effect on joint i. F_{ij}^q and F_{ij}^c are the rotation and centripetal elements of F_{ij}. β_{ij} is the angle between F_{ij} and its centripetal components. Based on the geometric of the joint, two angles $\alpha_i = const$ and $\gamma_i = const$ we have:

$$\varphi_i = \pi - \alpha_i - \gamma_i - \theta_i\,. \tag{5}$$

Consider the triangle $O_i A_1 A_2$, we can calculate the length of L_{i1} as:

$$L_{i1} = \sqrt{R_i^2 + r_i^2 - 2 R_i r_i \cos\varphi_i}\,. \tag{6}$$

In addition, we also have:

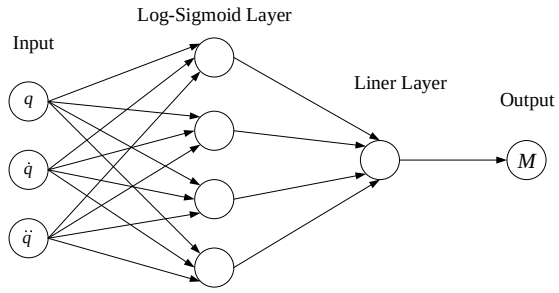

Figure 3. Neural network model.

$$r_i = \sqrt{L_{i1}^2 + R_i^2 - 2L_{i1}R_i \cos\beta_{i1}}\,. \tag{7}$$

Therefore:

$$\beta_{i1} = \arccos\frac{L_{i1}^2 + R_i^2 - r_i^2}{2L_{i1}R_i}\,. \tag{8}$$

As a result, the torque generated by the artificial muscle at i^{th} joint will be performed as follows:

$$M_{PAMi} = (F_{i1}\sin\beta_{i1} - F_{i2}\sin\beta_{i2})\,R_i\,. \tag{9}$$

3.2. Estimating the total torque applied to robot joints (M_{NN})

The developed rehabilitation robot system contains uncertainties in the system dynamic structure and parameters. Thus, the model-based calculation of applied joint torques (inverse dynamics) such as in [27] cannot improve the accuracy of torque estimations. However, Neural Networks are proved to be an efficient tool to approximate a wide variety of exciting functions [28]. Thus, in this paper, Neural Networks are used to estimate the total robot joint torques.

This research uses two independent neural networks for each hip and knee joint. As shown in the robot dynamic Equation (1), the joint torque is the function of joint acceleration, velocity, and position. Then, each neural network to estimate joint torque includes three inputs corresponding to the joint acceleration, velocity, and position. Moreover, each neural network has only one output corresponding to the estimated joint torque. In addition, each neural network includes two layers as follows:

- Layer 1: The transfer function is the logsig function, and the number of neurals is 4.
- Layer 2: The transfer function is the purely linear function, and the number of neurals is 1.
- The objective function is chosen as the difference between the actual and estimated output: $MSE = \frac{1}{n}\sum_{i=1}^{n}(y_i - \widehat{y}_i)^2$.
- The learning method is the back-propagation method Levenberg Marquardt.

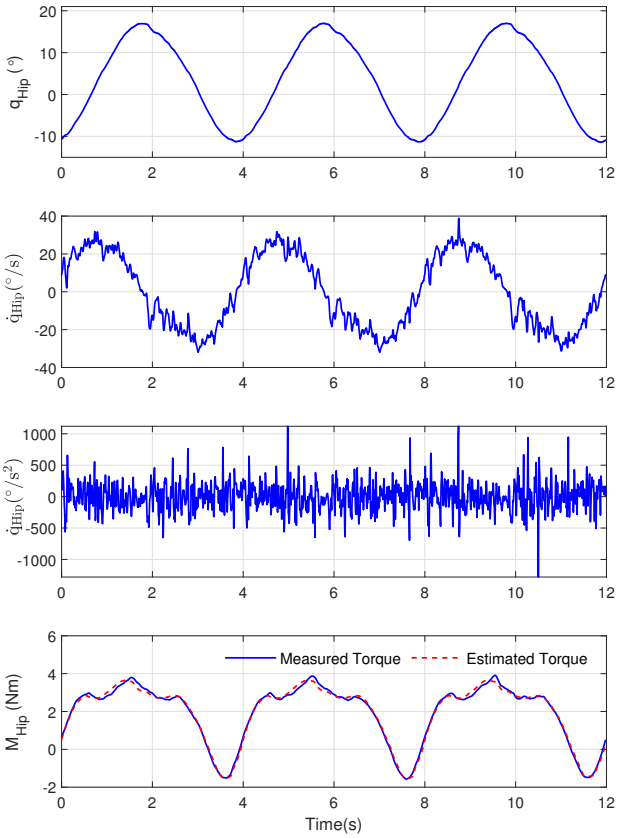

Figure 4. Sample input and output of the neural network for hip joint.

To obtain the training data of the neural network, the developed robot system is controlled to track the reference trajectory without a load (i.e. without rehabilitation object). Then, the torques generated by PAMs that affect robot joints are collected as output data. The actual joint acceleration, velocity, and position are collected as input data for the training. The sample input and output are shown in Figure 4 and Figure 5 for hip and knee joint, respectively.

Utilising the neural network toolbox in Matlab to train the proposed neural networks, we obtain the weight and bias coefficients for the two following networks. For the neural network that is used to estimate hip joint's torque:

$$w_{h1} = \begin{bmatrix} 0.2501 & -0.0160 & 0.0001 \\ 0.2824 & 0.0654 & -0.0004 \\ 0.7430 & -0.0194 & 0.0002 \\ 0.0337 & 0.0039 & 0.0000 \end{bmatrix},$$

$$b_{h1} = \begin{bmatrix} 0.7303 \\ 3.1417 \\ 8.0478 \\ -0.9932 \end{bmatrix},$$

$$w_{h2} = \begin{bmatrix} 3.4649 & 0.4422 & 2.7205 & 13.3358 \end{bmatrix},$$

$$b_{h2} = -6.5336\,.$$

For the neural network that is used to estimate knee joint's torque:

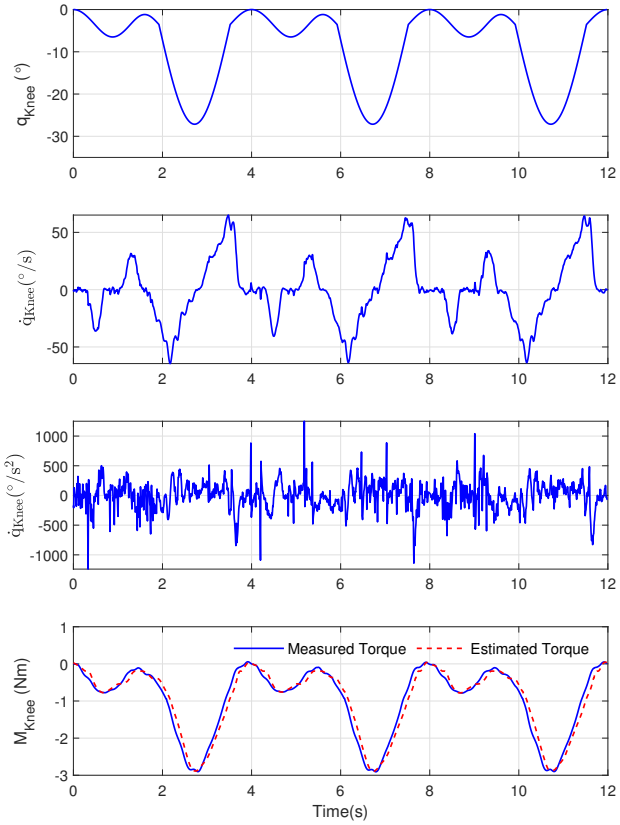

FIGURE 5. Sample input and output of the neural network for knee joint.

$$w_{k1} = \begin{bmatrix} -0.0814 & -0.0026 & -0.0000 \\ -0.0463 & -0.0455 & -0.0003 \\ -0.0786 & -0.0027 & -0.0000 \\ -0.0540 & 0.0419 & 0.0000 \end{bmatrix},$$

$$b_{k1} = \begin{bmatrix} -1.3038 \\ -0.1466 \\ -1.2532 \\ -0.1153 \end{bmatrix},$$

$$w_{k2} = \begin{bmatrix} -1.3840 & -1.1626 & -1.3612 & -1.0918 \end{bmatrix},$$

$$b_{k2} = 2.1821\,,$$

where w_{ij} and b_{ij} are the weight and bias of the neural network, with $i = h$ for hip, and $i = k$ for knee joint, $j = 1, 2$ represents the j^{th} layer of neurons.

Both fourth sub-figures of Figure 4 and Figure 5 show the estimated torques using a neural network in comparison to the actual torques. It can be seen that a precise approximation is obtained. The root mean square error (RMSE) is under 0.2 Nm for both joints. Hence, we can conclude that the estimation has a high accuracy. To verify the estimation's accuracy, the robot is operated in the trajectory tracking mode with a lower frequency (0.3 Hz). Both torques, including the estimation from NNs (M_{NN}) and inverse one (M_{INV}) computed from inverse dynamic Equation (1) are obtained for an analysis. As shown in Figure 6, in comparison to estimation using inverse dynamics

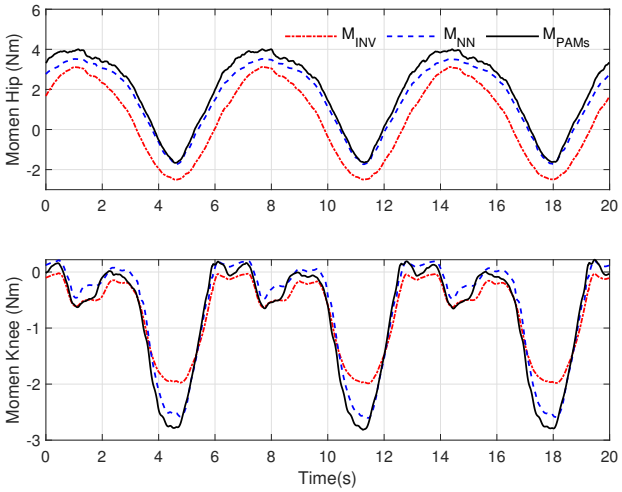

FIGURE 6. Comparison of the torque estimation results for neural network and inverse dynamic when tracking a 0.3 Hz gait patterns.

calculation, the estimation using a neural network achieves a much better precision. The high deviation in inverse dynamics calculation can be attributed to the fact that it cannot estimate the unknown component forces, such as friction, external disturbance, and other unmodelled dynamics.

3.3. ESTIMATION OF THE PATIENT'S RECOVERY

After determining the total applied torque M_{NN} and computing the torque generated by the PAMs (M_{PAM}), the external torques generated by the human can be calculated using Equation (4). This method allows for the easy estimation of the patient's recovery over time from the torques generated by the human. To verify the accuracy of this proposed method for estimating the torque generated by the patients, an experiment was conducted to estimate the torque generated by a load. In this experiment, a dumbbell was attached at the centre of mass of the robot's hip joint, and the robot was controlled to follow the reference gait trajectory at a frequency of 0.5 Hz. The moment of the dumbbell can be quickly obtained through the joint angle and distance from its position to the rotation point. This information can then be used to calculate the external torque generated by the load and to validate the accuracy of the proposed method for estimating the torque generated by a patient during rehabilitation.

Figure 7 show that the estimation of the torque generated by the dumbbell is highly accurate, with RMSE is under 0.26 Nm. Although the error is still there, it is inevitable when we depend on the theoretical model for the estimation and verification. Positive dumbbell estimation results make it possible to estimate the patient's rehabilitation (also known as the torque estimate of the human muscle). The following section will use the patient's recovery estimate to control the gait training robot.

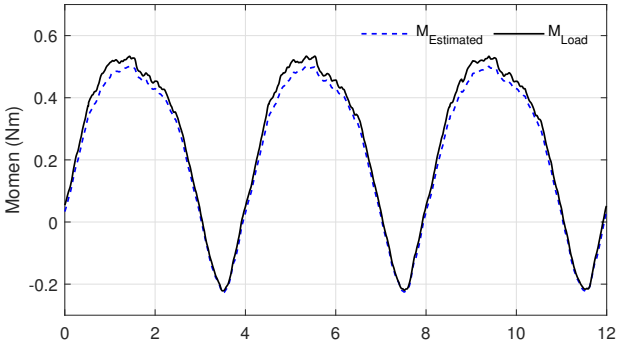

Figure 7. Estimation verification with the external load is a 5 kg-dumbbell.

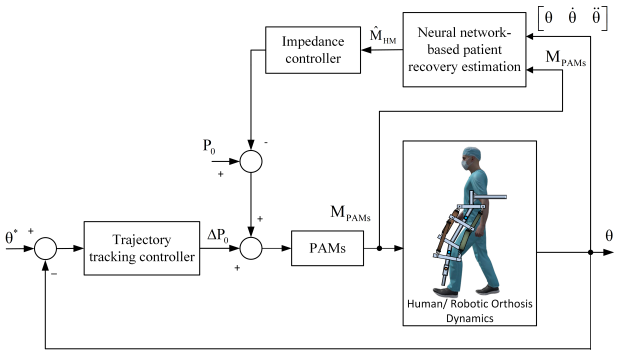

Figure 8. The neural network-based impedance control diagram of gait training robot.

3.4. Robot impedance control

One of the essential criteria of a rehabilitation robot is its stiffness, or impedance. The nominal pressure supply to the antagonistic actuator's two PAMs determines its stiffness property. This study employs the stiffness-nominal pressure relationship presented by Choi et al. [29]. The compliance γ_i of an antagonistic actuator driven by PAMs is calculated as follows:

$$\gamma_i = \frac{\theta_i}{2r^2 K_{0i}\theta_i + K_{1i}(r^2\pi P_{0ei} - P_{efi}x_{ei}r) + K_{1i}r^2\Delta P_i}, \quad (10)$$

where γ_i is the compliance of joint i, ΔP_i represents the pressure values that can be controlled in the pneumatic artificial muscles (PAMs), which are considered as arbitrary functions of time. The symbol r is used to denote the radius of the disks for the hip and knee joints in the robotic gait training orthosis; K_{0i} and K_{1i} are parameters of the PAM numerical model (see Table 2), x_{ei} as the PAM length is expressed in θ_i, and P_{0ei} and P_{efi} are the nominal pressures for extension PAM and the difference in nominal pressures for the PAMs powering hip and knee sagittal plane joints, respectively.

Actuators	K_{0i} [N]	K_{1i} $[\frac{\text{N}}{100\text{kPa}}]$
Hip PAMs	0.691	1.096
Knee PAMs	0.572	0.835

Table 2. The spring parameters of the used PAMs.

Figure 8 depicts the robotic orthosis' impedance control design. The external force effect to the robot F_{ex} can be used to control the robot's impedance. The notion of robotic orthosis impedance control is to set the robot impedance high (low compliance) if the external force opposes the rotating movement (prevents movement). In the opposite situation, if the external torque supports the robot's movement, the robot's impedance is reduced. The following equation represents the impedance controller's control signal.

$$\Delta P_{0i,t} = \begin{cases} K_{ui}M_{estimated}, & \text{if } M_{estimated} > 0 \\ 0, & \text{otherwise} \end{cases}, \quad (11)$$

where K_{ui} is the positive gain that is tuned based on the initial pressure P_{0i} and the estimation torque $M_{estimated}$. Since the impedance controller only increases joint compliance, the initial state of the robot is set with the maximum impedance that strictly guides the patient to designate trajectories. For the safety requirement, the initial pressure of PAMs is the upper limit of the impedance controller's control signal. In addition, an adaptive sliding mode control is inherent from previous research in [30] for a trajectory tracking purpose.

4. Experiments and results

4.1. Experiment Setup

To evaluate the effectiveness of the controller when adding an estimate of the patient's recovery, we used two bicycle tubes attached to the hip and knee joints for creating cycling forces. The test process to evaluate the control quality in this research is based on the set trajectory. The signals for the robot joints are taken according to the sample trajectory of the human foot with maximum elasticity: $-12°/-17°$ for the hip joint and $-29°/-0°$ for the knee joint. The controller's sampling time is 5 ms. The actual image of the experimental setup is given in Figure 9. The robot is set to trajectory tracking mode in the experiment's first phase. In the second step, the impedance control is turned on to regulate the robot joint compliance after the system is stable. During experiments, data on each joint's desired, measured trajectories and compliance are gathered for evaluation.

4.2. Experimental results

The mean of all observed trajectories is derived first to evaluate the system's performance in trajectory tracking mode. The maximum tracking error (MTE) and root mean square tracking error (RMSTE) between the measured and intended trajectories are then determined and presented in Table 3. Figure 10 depicts the tracking performances of the BK-Gait robot

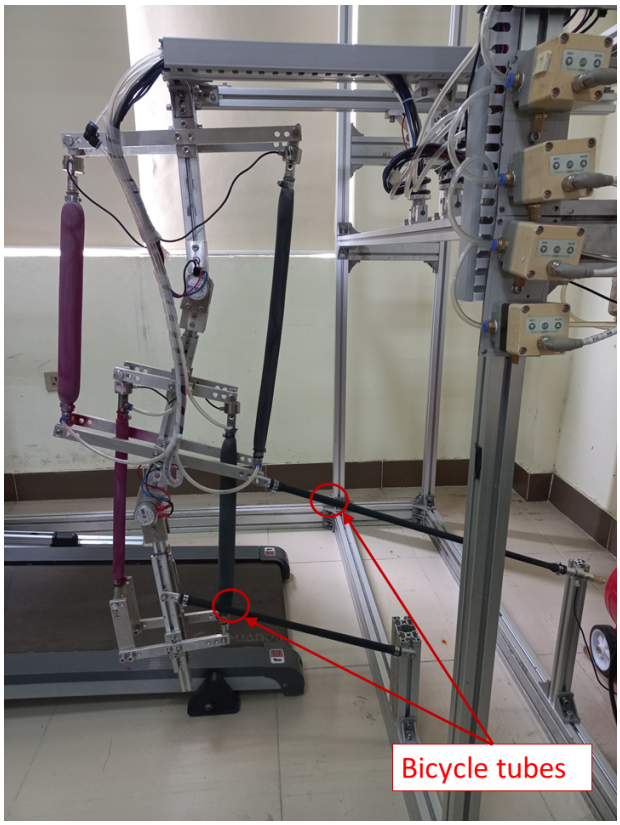

FIGURE 9. Experimental platform.

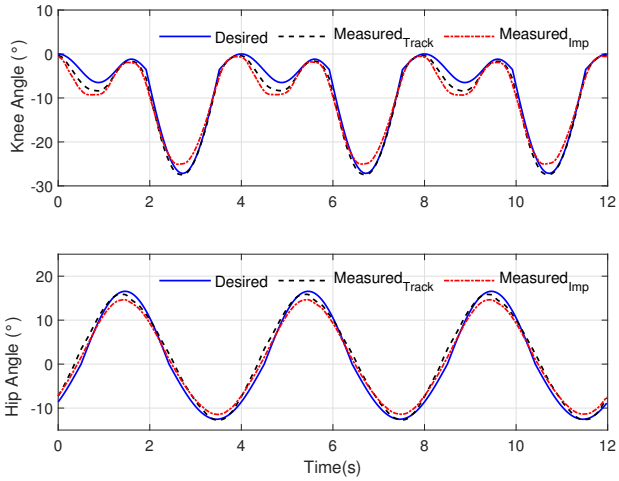

FIGURE 10. Tracking performance of the BK-Gait robot when operating in trajectory tracking and impedance control mode. The blue line is the desired trajectory. The black dash line and dash-dot red line represent the measured trajectories in trajectory tracking and impedance control mode, respectively.

in both trajectory tracking and impedance control modes. We can see that the robot always tracks the desired trajectory in both operating modes. In detail, the MTE and RMSTE are below 3.35° for both hip and knee joints in trajectory tracking mode. The tracking performance is somewhat decreased in the impedance control mode, with MTE = 5.91° and RMSTE = 2.89°. It commonly happens in rehabilitation robots, allowing patients to be more confident in impedance control mode. In comparison to the similar configuration PAM-based robot orthosis in [8, 27], the BK-Gait robot achieves an equivalent trajectory tracking performance in the impedance control mode. For example, the MTE of the Airgait in [8] is about 6.81° and the 7-DOF robot's MTE [8] is less than 15°.

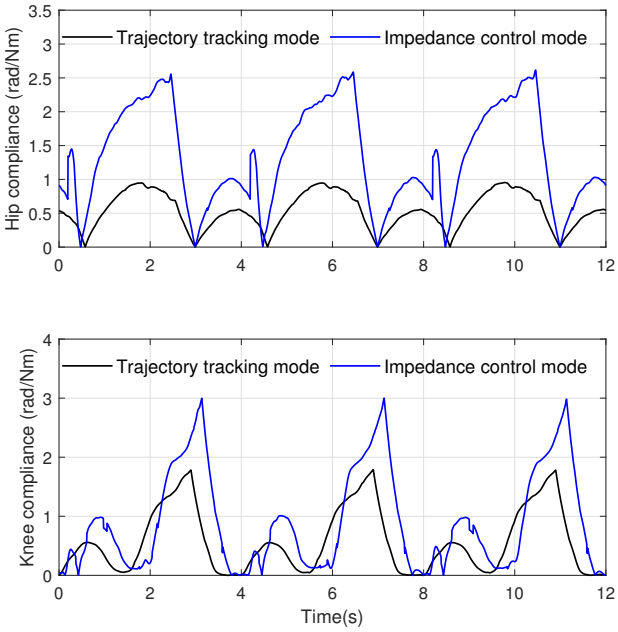

FIGURE 11. Joint compliance of the robot in trajectory tracking and impedance control mode.

Parameter	Trajectory tracking control		Impedance control	
	Hip	**Knee**	**Hip**	**Knee**
MTE [°]	2.2	3.4	3.6	5.9
RMSTE [°]	1.2	1.8	1.8	2.9
Max compliance [Rad·Nm^{-1}]	0.9	1.8	2.7	3.0

TABLE 3. Experimental evaluation.

Figure 11 shows the robot joints' compliances in both scenarios of the experiment. When the robot is set for trajectory tracking purposes with a high impedance, the joints' compliances reach 0.92 rad·Nm^{-1} for the hip joint and 1.83 rad·Nm^{-1} for the knee joint. When the impedance control mode is enabled, the robot compliance increases to 2.69 rad·Nm^{-1} and 3.01 rad·Nm^{-1} for the hip and knee joints, respectively, in response to the external force from the tubes. While the tracking controller remains steady, the impedance controller may modify its joint compliance to the patient recovery represented by the external force. The impedance controller performs effectively when adapting the joints' compliances to the external force representing the human effort. We can observe that the joints' compliance changes are

similar to the two counter systems reported in [8, 27].

5. Conclusion

In this paper, a neural network-based method was proposed to estimate the patient's recovery, an important factor for a gait training robot system powered pneumatic artificial muscles. Since the robot system operates at a slow velocity range, the neural network structure can be kept simple, and the training data can be collected without the need for measuring external forces, making it easy to implement in practice with highly accurate estimation. The estimated patient recovery is then used for the impedance control of the gait training robot system, leading to improved joint compliance coefficients, which make patients more comfortable and confident in performing rehabilitation exercises. In the future, the developed system will be tested with real human subjects to evaluate its effectiveness in practice. Overall, this study offers a promising approach for enhancing the rehabilitation process and improving the quality of life for patients.

Acknowledgements

This research is funded by Hanoi University of Science and Technology (HUST) under project number T2022 – PC – 002.

References

[1] M. Kyrarini, F. Lygerakis, A. Rajavenkatanarayanan, et al. A survey of robots in healthcare. *Technologies* **9**(1):8, 2021. https://doi.org/10.3390/technologies9010008

[2] G. Morone, S. Paolucci, A. Cherubini, et al. Robot assisted gait training for stroke patients: Current state of the art and perspectives of robotics. *Neuropsychiatric disease and treatment* **13**(1):1303–1311, 2017. https://doi.org/10.2147/NDT.S114102

[3] D. B. Reynolds, D. W. Repperger, C. A. Phillips, G. Bandry. Modeling the dynamic characteristics of pneumatic muscle. *Annals of Biomedical Engineering* **31**(3):317–319, 2003. https://doi.org/10.1114/1.1554921

[4] C.-P. Chou, B. Hannaford. Measurement and modeling of McKibben pneumatic artificial muscles. *IEEE Transactions on Robotics and Automation* **12**(1):90–102, 1996. https://doi.org/10.1109/70.481753

[5] T.-Y. Choi, J.-J. Lee. Control of manipulator using pneumatic muscles for enhanced safety. *IEEE Transactions on Industrial Electronics* **57**(8):2815–2825, 2010. https://doi.org/10.1109/TIE.2009.2036632

[6] X. Cheng, Y. Zhou, C. Zuo, X. Fan. Design of an upper limb rehabilitation robot based on medical theory. *Procedia Engineering* **15**:688–692, 2011. https://doi.org/10.1016/j.proeng.2011.08.128

[7] L. Zhao, H. Cheng, Y. Xia, B. Liu. Angle tracking adaptive backstepping control for a mechanism of pneumatic muscle actuators via an AESO. *IEEE Transactions on Industrial Electronics* **66**(6):4566–4576, 2019. https://doi.org/10.1109/TIE.2018.2860527

[8] Q.-T. Dao, S.-i. Yamamoto. Assist-as-needed control of a robotic orthosis actuated by pneumatic artificial muscle for gait rehabilitation. *Applied Sciences* **8**(4):499, 2018. https://doi.org/10.3390/app8040499

[9] M.-C. Trinh, T.-H. Do, Q.-T. Dao. Development of a rehabilitation robot: Modeling and trajectory tracking control. *ASEAN Engineering Journal* **12**(4):121–129, 2022. https://doi.org/10.11113/aej.v12.17196

[10] P. Beyl, M. Van Damme, R. Van Ham, et al. Pleated pneumatic artificial muscle-based actuator system as a torque source for compliant lower limb exoskeletons. *IEEE/ASME Transactions on Mechatronics* **19**(3):1046–1056, 2014. https://doi.org/10.1109/TMECH.2013.2268942

[11] C.-T. Chen, W.-Y. Lien, C.-T. Chen, et al. Dynamic modeling and motion control of a cable-driven robotic exoskeleton with pneumatic artificial muscle actuators. *IEEE Access* **8**:149796–149807, 2020. https://doi.org/10.1109/ACCESS.2020.3016726

[12] Z. Q. Tang, H. L. Heung, X. Q. Shi, et al. Probabilistic model-based learning control of a soft pneumatic glove for hand rehabilitation. *IEEE Transactions on Biomedical Engineering* **69**(2):1016–1028, 2022. https://doi.org/10.1109/TBME.2021.3111891

[13] C. M. Thalman, M. Debeurre, H. Lee. Entrainment during human locomotion using a soft wearable ankle robot. *IEEE Robotics and Automation Letters* **6**(3):4265–4272, 2021. https://doi.org/10.1109/LRA.2021.3066961

[14] Q.-T. Dao, V.-V. Dinh, M.-C. Trinh, et al. Nonlinear extended observer-based ADRC for a lower-limb PAM-based exoskeleton. *Actuators* **11**(12):369, 2022. https://doi.org/10.3390/act11120369

[15] Y. Wang, Q. Xu. Design and testing of a soft parallel robot based on pneumatic artificial muscles for wrist rehabilitation. *Scientific Reports* **11**:1273, 2021. https://doi.org/10.1038/s41598-020-80411-0

[16] P. Ohta, L. Valle, J. King, et al. Design of a lightweight soft robotic arm using pneumatic artificial muscles and inflatable sleeves. *Soft Robotics* **5**(2):204–215, 2018. https://doi.org/10.1089/soro.2017.0044

[17] A. Colomé, D. Pardo, G. Alenyà, C. Torras. External force estimation during compliant robot manipulation. In *2013 IEEE International Conference on Robotics and Automation*, pp. 3535–3540. 2013. https://doi.org/10.1109/ICRA.2013.6631072

[18] E. Berger, S. Grehl, D. Vogt, et al. Experience-based torque estimation for an industrial robot. In *2016 IEEE International Conference on Robotics and Automation (ICRA)*, pp. 144–149. 2016. https://doi.org/10.1109/ICRA.2016.7487127

[19] A. Wahrburg, E. Morara, G. Cesari, et al. Cartesian contact force estimation for robotic manipulators using Kalman filters and the generalized momentum. In *2015 IEEE International Conference on Automation Science and Engineering (CASE)*, pp. 1230–1235. 2015. https://doi.org/10.1109/CoASE.2015.7294266

[20] Y. Lu, Y. Shen, C. Zhuang. External force estimation for industrial robots using configuration optimization. *Automatika* **64**(2):365–388, 2023. https://doi.org/10.1080/00051144.2023.2166451

[21] A. C. Smith, F. Mobasser, K. Hashtrudi-Zaad. Neural-network-based contact force observers for haptic applications. *IEEE Transactions on Robotics* **22**(6):1163–1175, 2006. https://doi.org/10.1109/TRO.2006.882923

[22] N. Yilmaz, J. Y. Wu, P. Kazanzides, U. Tumerdem. Neural network based inverse dynamics identification and external force estimation on the da Vinci research kit. In *2020 IEEE International Conference on Robotics and Automation (ICRA)*, pp. 1387–1393. 2020. https://doi.org/10.1109/ICRA40945.2020.9197445

[23] Z. Chua, A. M. Okamura. Characterization of real-time haptic feedback from multimodal neural network-based force estimates during teleoperation. In *2022 IEEE/RSJ International Conference on Intelligent Robots and Systems (IROS)*, pp. 1471–1478. 2022. https://doi.org/10.1109/IROS47612.2022.9981662

[24] J. Y. Wu, N. Yilmaz, U. Tumerdem, P. Kazanzides. Robot force estimation with learned intraoperative correction. In *2021 International Symposium on Medical Robotics (ISMR)*, pp. 1–7. 2021. https://doi.org/10.1109/ISMR48346.2021.9661568

[25] M. Chiako, B. Mahdi, A. Vahid. Muscle force estimation from lower limb EMG signals using novel optimised machine learning techniques. *Medical and Biological Engineering and Computing* **60**(3):683–699, 2022. https://doi.org/10.1007/s11517-021-02466-z

[26] B. Siciliano, L. Sciavicco, L. Villani, G. Oriolo. *Robotics: Modelling, Planning and Control*. Springer London, London, 1st edn., 2009.

[27] S. Hussain, S. Q. Xie, P. K. Jamwal. Adaptive impedance control of a robotic orthosis for gait rehabilitation. *IEEE Transactions on Cybernetics* **43**(3):1025–1034, 2013. https://doi.org/10.1109/TSMCB.2012.2222374

[28] R. Uhrig. Introduction to artificial neural networks. In *Proceedings of IECON '95 – 21st Annual Conference on IEEE Industrial Electronics*, vol. 1, pp. 33–37. 1995. https://doi.org/10.1109/IECON.1995.483329

[29] T.-Y. Choi, J.-J. Lee. Control of manipulator using pneumatic muscles for enhanced safety. *IEEE Transactions on Industrial Electronics* **57**(8):2815–2825, 2010. https://doi.org/10.1109/TIE.2009.2036632

[30] Q.-T. Dao, V. V. Dinh, C. T. Vu, et al. An adaptive sliding mode controller for a PAM-based actuator. *Engineering, Technology and Applied Science Research* **13**(1):10086–10092, 2023. https://doi.org/10.48084/etasr.5539